XLIII CILAMCE
21–25, November, 2022
FOZ DO IGUAÇU – PR – BRAZIL

The influence of non-isothermal flows in the Taylor-Couette instability through numerical analysis

André Y. K. Kamiya[1], Henrique Q. Rodrigues[1], Julien Pellé[2], Thiago Antonini Alves[3], Fernando Augusto Alves Mendes[1], Augusto Salomão Bornschlegell[1]

[1]*Faculty of Engineering, University of Grande Dourados*
Rodovia Dourados - Itahum, km 12 - Cidade Universitária, 79804970, Mato Grosso do Sul, Brazil
andre.kamiya705@academico.ufgd.edu.br, henrique.rodrigues062@academico.ufgd.edu.br,
fernandomendes@ufgd.edu.br, augustosalomao@ufgd.edu.br
[2]*Laboratory of Automation, Mechanics and Industrial and Human Computer Science, Université Polytechnique Hauts-de-France*
Campus Mont Houy, 59313 Valenciennes cedex 9, France
jpelle@uphf.fr
[3]*Dept. of Mechanical Engineering, Federal University of Technology – Paraná*
R. Doutor Washington Subtil Chueire, 330 - Jardim Carvalho, 84017-220, Ponta Grossa - PR, Brazil
antonini@utfpr.edu.br

Abstract. The Taylor-Couette flow is a classic rotational flow studied since the beginning of the 20th century. The phenomenon occurs in the gap between two cylinders with different rotational velocities. It happens when one of the cylinders, usually the inner one, has a rotation that causes centrifugal forces higher than the viscous forces. The most recognizable characteristic of the flow is the Taylor vortex, an eddy-like pattern that appears across the cylinders length. The present simulation of Taylor-Couette in the gap inside an electric machine considers an aspect ratio air gap - cylinder length of 1:20 and the radius rate of 0.9859. The present work evaluates the necessary rotation, under the geometric conditions presented, to form the Taylor vortices in isothermal flow and when the flow is submitted to temperature gradients. The GCI method is used to validate the grid dependency. We have observed and discussed the sensibility of temperature gradients to the identification of the critical flow, to the velocity field and to the torque at the outer cylinder.

Keywords: Taylor-Couette, CFD, Instability, OpenFOAM

1 Introduction

The Taylor-Couette flow is a common rotational flow potentially found in any gap between concentric cylinders at different rotational speeds. This flow pattern appears when, for instance, the outer cylinder is steady and the inner cylinder rotation is high enough to generate the instability in the flow. If the rotation of the inner cylinder induces a centrifugal force higher than the viscous forces acting on the walls, it causes the formation of vortex patterns, called Taylor vortices or Taylor instabilities. In this phenomenon, the Taylor vortices are counter-rotating structures, as shown in Fig. 1. The presence of the Taylor vortices does not necessary imply in a turbulent flow. Initially, these structures present a stable pattern and are laminar.

Since the initial article about the phenomenon published by Taylor [1], there has been many studies regarding the flow's nature. Monico et al. [2] and van Gils et al. [3] studies are some recent examples of more complex and extensive analysis, examining the effects of the turbulence caused by high Reynolds and Taylor numbers. In laminar studies, Abdelali et al. [4] presented a controlling technique for Taylor-Couette flow formation.

There are also applied researches in processes which involves tools with a rotating component. Pawar and Thorat [5] studied the effects of the flow in a heat exchanger with a scrapped surface, which had a better convergence using the k-ϵ turbulence model of simulation. Park et al. [6] used the flow to analyze the stability of oxygen emulsion in a bioreactor. Curran and Black [7] tested the instability in the aggregation and breakage processes.

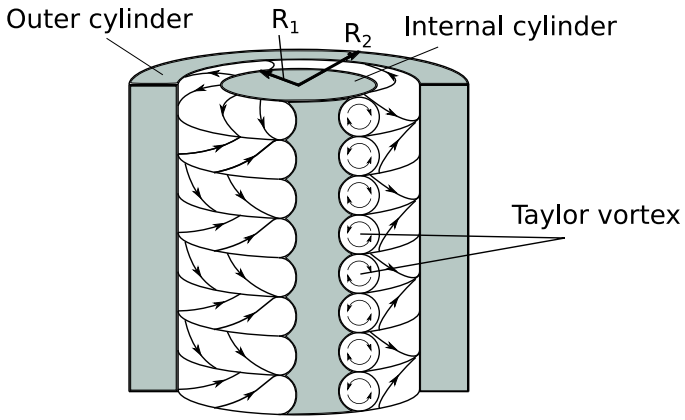

Figure 1. Representation of the vortices' orientation in the Taylor-Couette flow

The advance of computing technology have been improving numerical simulations of fluids, creating many possible options of flow configurations, some of which can more accurately show the effects of Taylor-Couette flow. Paghdar et al. [8], Pirrò and Quadrio [9] and Viazzo and Poncet [10], for example, used direct numerical simulations to analyze their respective topics. Mahmoudirad et al. [11] used pisoFoam solver to simulate a laminar flow with periodic oscillation in a 14.5 mm gap. Dubas et al. [12] tested two different turbulence models in the simulation of a rim drive thruster: RNG $k-\epsilon$ and $k-\omega$ SST. The k-omega model led to the better results.

This paper presents the numerical simulation of the Taylor-Couette critical flow applied to the study of the air gap between the rotor and the stator of electric machines. More precisely, we investigate the conditions for the Taylor Vortices formation and the influence of the temperature in this process.

2 Methodology

In order to evaluate the relation between centrifugal and viscous forces, a non-dimensional value called Taylor number (Ta) is used. Ta can be calculated in various manners and in this work, we use the definition stated by Hosain et al. [13], used for flows in which only the inner cylinder rotates:

$$Ta = \Omega^2 R_m (R_2 - R_1)^3 / \nu^2 \tag{1}$$

As shown, this parameter is related to the rotation speed (Ω, rad/s), the radius of the apparatus (R, m) and the kinematic viscosity (ν, m^2/s) of the fluid used. The Taylor instabilities start to occur when Ta is greater than the Critical Taylor number (Ta_{cr}), also defined in Hosain et al. [13]:

$$Ta_{cr} = \pi^4 \left(1 - \frac{R_2 - R_1}{2R_m}\right)^{-2} \left(0.0571 \left[1 - 0.652\frac{R_2 - R_1}{R_1}\right] + 0.00056 \left[1 - 0.652\frac{R_2 - R_1}{R_1}\right]^{-1}\right)^{-1} \tag{2}$$

Another non-dimensional number used in studies of the flow instability is the Reynolds number, calculated using the following equation, where V is the linear velocity of the inner rotor ($V = \Omega \times R_1$):

$$Re = \frac{V(R_2 - R_1)}{\nu} \tag{3}$$

There are also the geometric characteristics of aspect ratio ($\Gamma = (R_2 - R_1)/L$), in which L is the length of the machine, and radius rate ($\eta = R_1/R_2$) used to quickly discern different scales of Taylor-Couette flow.

2.1 Geometry and boundary conditions

Due to the flow symmetric behavior, just part of the annular domain was modeled. A three dimensional 15° section of the circular region between the inner and outer cylinder was created using the blockMesh mesher

from OpenFOAM v9. The mesh is built with 258944 hexahedral cells. The geometry is modeled with a 1/24th symmetry section to ease the computational cost. The face patches that represent the symmetry were modeled as cyclical boundary condition, so it can function as a full circumference flow, properly presenting the phenomenon. The inner cylinder's face is set to rotate in the selected speed, while the other lateral faces are set as walls with the "noslip" boundary condition. The upper and lower axial boundaries are of the type wall. All walls are considered to be smooth.

The geometry is approximated to that of an electrical machine. The dimensions used are $R_1 = 0.07$ m, $R_2 = 0.071$ m, therefore the studied case has a gap of 0.001 m, and the axial length of the rotor is $L = 0.02$ m. The chosen parameters result in the non-dimensional numbers of $\Gamma = 20$ and $\eta = 0.9859$.

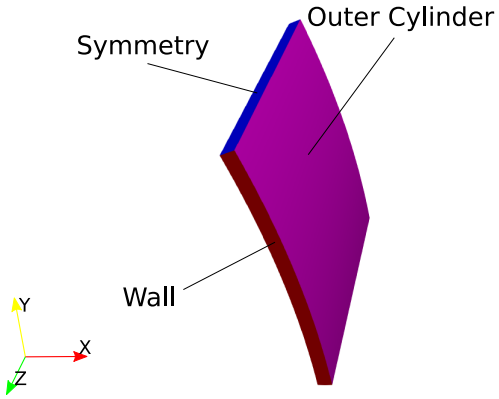

(a) Exterior of the simulated section

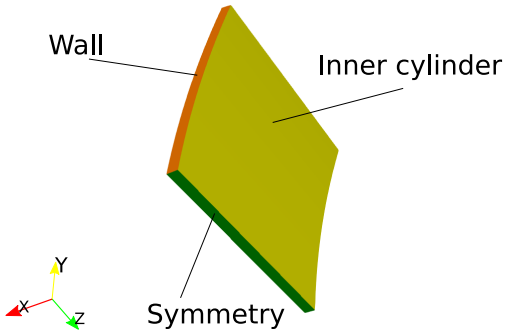

(b) Interior of the simulated section

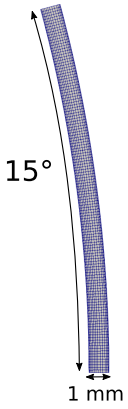

(c) 2D view of the side

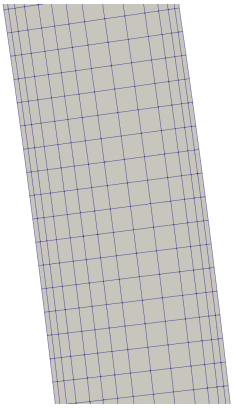

(d) Zoom of the mesh

Figure 2. Numerical domain of the studied section

2.2 Isothermal flow numerical model

The turbulence model used in the isothermal problem is $k - \omega$ (SST). This is a two equation model which uses turbulence kinetic energy (k) and turbulence specific dissipation rate (ω) to accomplish the simulation. k and ω are defined by the size of the gap, velocity of the rotor and the turbulence intensity, here arbitrated as 5%.

The isothermal simulations are done using pisoFoam, a transient incompressible flow URANS solver. The algorithms used were GAMG with 10^{-6} of tolerance for pressure and smoothSolver with 10^{-5} of tolerance for the other parameters.

The integration in time is numerically calculated using the backward algorithm, a implicit second order time scheme. The gradient scheme used is Gauss linear and the divergence scheme is Gauss limitedLinear, which is a second order discretization. The relaxation factor used is 0.7 for both pressure and velocity. The simulated flow has a density of $\rho = 1$ kg/m^3 and viscosity of $\nu = 10^{-5}$ m^2/s.

2.3 Grid independency

To make sure that the results do not depend on mesh refinement, we applied the GCI grid dependency method, the same used in Celik et al. [14]. The method consists in three different meshes with different amounts of cells and comparing them through the methods' criteria.

An arbitrary ϕ parameter is chosen to compare the three grids. The grids have a proportion (r) of 1.3 between them, a value found in the experiences of Celik et al. [14] using the GCI method. The difference of ϕ between two grids is used to generate new extrapolated values of ϕ. Those new parameters are used in a sequence of equations that result in a value (GCI) that suggests the independence of the grids.

Here, the parameter used to calculate the grid dependency is the dimensionless torque (G), found in Martínez-Arias et al. [15] as: $G = t/(2\pi\rho\nu^2 L)$. Where t is the dimensional torque (N). More specifically, the value of ϕ is the average G between 0.2 and 1 second.

The ϕ parameters were calculated for the isothermal case of Re = 595. The reference parameters are $\phi_1 =$ 6724296.34, $\phi_2 =$ 6891409.03 and $\phi_3 =$ 6947113.26.

Table 1. Parameters and results of GCI equations

Mesh size	ϕ	GCI_{32}	GCI_{21}
$N_1 = 575244$	$\phi_1 = 6724296.34$	$r_{32} = 1.3$	$r_{21} = 1.3$
$N_2 = 258944$	$\phi_2 = 6891409.03$	$GCI_{32} = 1.5\%$	$GCI_{21} = 0.5\%$
$N_3 = 116699$	$\phi_3 = 6947113.26$		

The table indicates the characteristics of the meshes in the first two columns. GCI_{32} represent the GCI value comparing mesh 2 to mesh 3. The same is done in GCI_{21}, but with meshes 1 and 2. The low GCI in both comparisons show that there is little uncertainty between the respective grids, which demonstrates that the results presents weak dependency on further mesh refinement. Then, we used the N_2 grid for all the following simulations.

2.4 Thermal numerical model

We used the buoyantPimpleFoam solver, normally used in transient and compressible cases, but in this study, it will be used primarily to showcase the effects of the temperature gradient in the system. The other necessary settings are the same as the ones used for the isothermal cases.

Here, we chose two different temperatures in the inner cylinder: 400 and 500 K. The outer cylinder has 300 K in both cases.

3 Results

3.1 Isothermal formation of Taylor-Couette

Using the eq. 2, the critical value of the Taylor number is approximately 1729. Therefore, the early formations of the Taylor-Couette instabilities can, according to the equation, be found around 49 rad/s ($Re = 343$). Following this reference value, we tested the initial parameter of $Re = 350$ and then also tested some other rotations around it. The Fig. 3 demonstrates the results of those tests.

The $Re = 336$ result has the usual laminar Couette formation, with a gradient of velocity from the inner cylinder to the outer cylinder changing in a linear manner across the gap between cylinders. The $Re = 350$ result presents, in addition to the wall effect on the corners also present for Re=336, the first sign of the TC vortices formation, starting from both extremities of the cylinder axis. The flow with $Re = 364$ presents more of the expected characteristics of a Taylor-Couette, however it can't generate all the vortices in the entire cylinder axis length. The $Re = 378$ has the fully formed laminar Taylor-Couette flow, with all 10 vortices. The last two vortices start to appear between 0,6 and 0,7 second and has a more defined look after around 0,9 second.

The graph seen in Fig. 4 illustrates the Torque of each rotation through time. In the cases that represent the early stages of Taylor-Couette formation, it shows little increment of torque after the flow stabilizes at around 0,18 second. The flow with $Re = 378$ continues to increase its torque after 0.18 second, indicating the higher forces caused by the instabilities created.

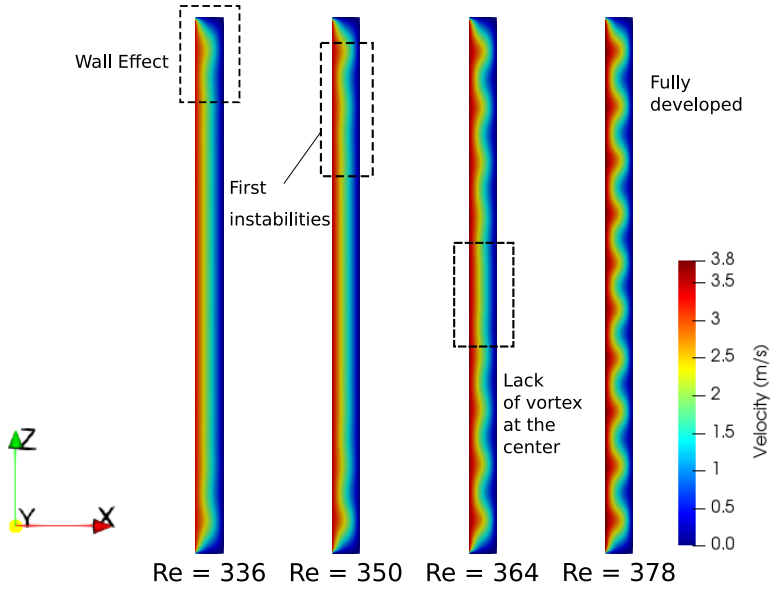

Figure 3. Results of the simulations in the indicated Reynolds number.

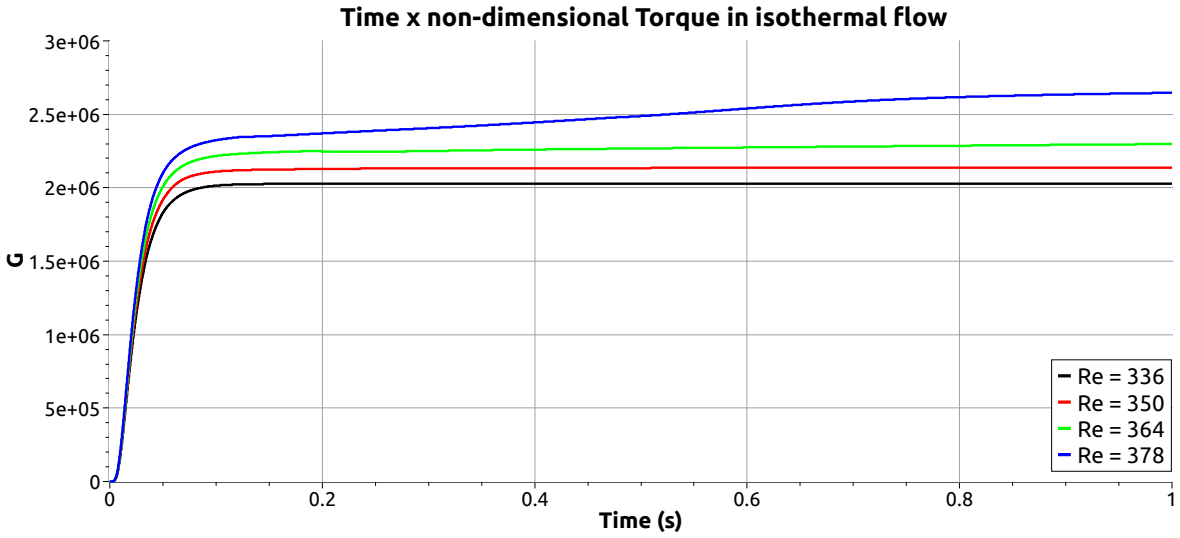

Figure 4. Torque comparison of the simulated isothermal flows

3.2 Thermal formation of Taylor-Couette

The new thermal conditions applied to the studied case delayed the Taylor-Couette vortices formation to a higher rotation. As illustrated in Fig. 5, the initial vortices in the $400K$ and $500K$ simulations at around $Re = 560$ and $Re = 574$ respectively. The fully formed Taylor-Couette flow can be seen at $Re = 595$ and $Re = 609$. There is also a change in the quantity of vortices formed in the $500K$ case during the 1 second simulated, now generating 9 vortices, different from the 10 vortices in the isothermal results.

We notice that, initially, the instability formation in the thermal cases starts from the extremities just like in the isothermal problem. Nevertheless, the instability propagation in the thermal problems arises all over cylinder's length, from the inner to the outer radius, at the later stages. This can be observed in $Re = 574$ for the 400 K case and $Re = 588$ for the 500 K, which shows a patterns different from the isothermal $Re = 364$, characterized by the lack of significant vortices at the center of the domain. The thermal simulations stabilize after 0.3 second.

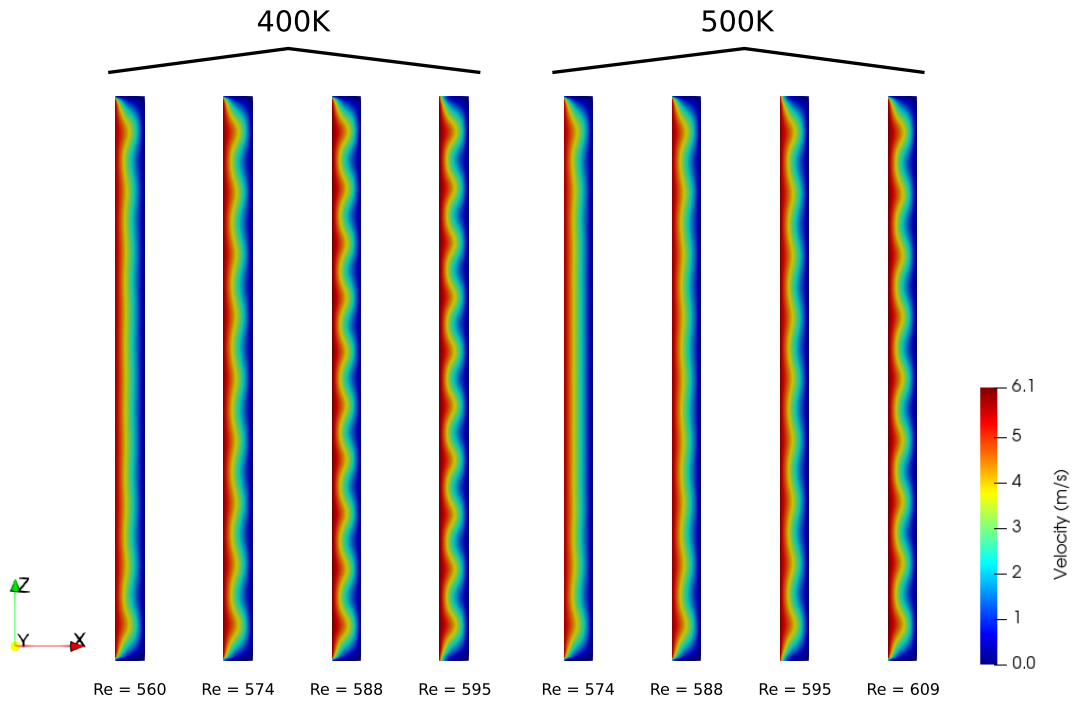

Figure 5. Results of both thermal simulations in the indicated Reynolds number

3.3 The torque parameter under the thermal conditions

The TC instability for the thermal problems was noticed only at higher rotations. Consequently, the torque is also higher. In Fig. 6 we compare the torque behavior over time for the three fully developed cases (Isothermal and Re=378; T=400 K and Re=595; T=500 K and Re=609) and also for the isothermal case at Re=595.

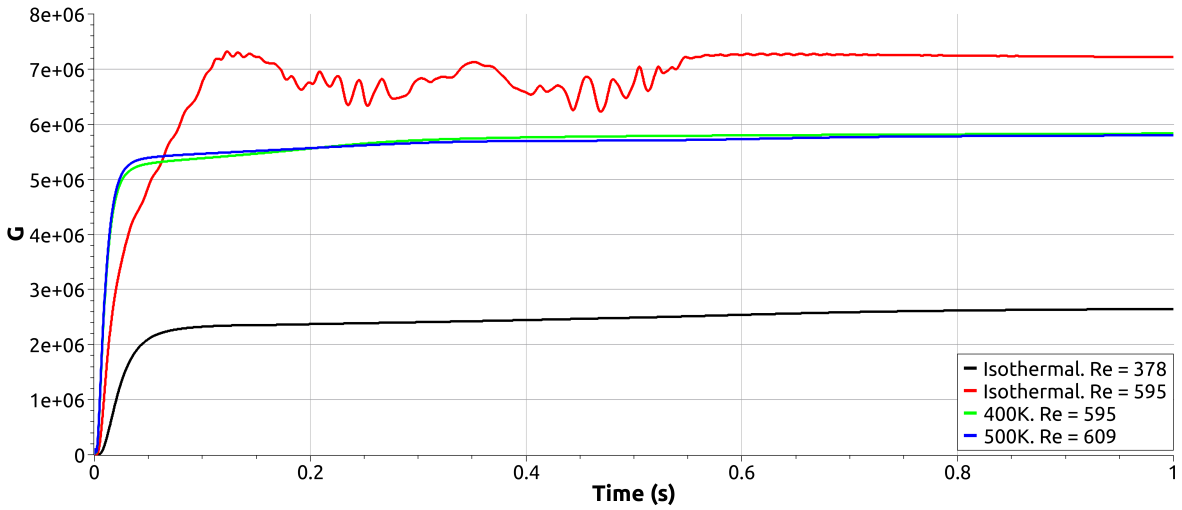

Figure 6. Torque comparison of the fully-formed flows

In addition to the difference in magnitude, the manner in which torque G increases over time also changes. The thermal cases show the earliest growth of G, reaching 5e+6 at around 0.02 second and changing to a lower increase per time. The isothermal case of $Re = 595$ takes around 0.05 second to lower its increase rate.

The isothermal case of $Re = 595$, which is in the turbulent regime of the Taylor-Couette flow, has a higher

value of G compared to the thermal cases. This suggests that the change in flow regime has a significant impact in determining the magnitude of G in the flow.

4 Conclusions

The results found in this study present significant difference in the Taylor-Couette flow formation for the isothermal and thermal models. This difference can be noticed in the necessary rotational speed of the inner cylinder for the surge of vortices and for the visual characteristics of the instability formation. The Taylor-Couette flow is found at Re=378 for the isothermal model and, for the thermal cases, at around Re=600. Then, higher rotational speeds are necessary to initiate the TC instability when heat transfer is present.

Authorship statement. The authors hereby confirm that they are the sole liable persons responsible for the authorship of this work, and that all material that has been herein included as part of the present paper is either the property (and authorship) of the authors, or has the permission of the owners to be included here.

References

[1] G. Taylor. Stability of a viscous liquid contained between two rotating cylinders. *Philosophical Transactions of the Royal Society of London*, vol. 223, pp. 289–343, 1923.
[2] R. O. Monico, van der E. P. Poel, R. Verzicco, S. Grossmann, and D. Lohse. Boundary layer dynamics at the transition between the classical and the ultimate regime of taylor-couette flow, 2013.
[3] van D. P. M. Gils, S. G. Huisman, S. Grossmann, C. Sun, and D. Lohse. Optimal taylor-couette turbulence, 2011.
[4] A. Abdelali, H. Oualli, A. Rahmani, B. Merzkane, and A. Bouabdallah. Experiment and numerical simulation of taylor–couette flow controlled by oscillations of inner cylinder cross section. *Journal of the Brazilian Society of Mechanical Sciences and Engineering*, vol. 41, n. 6, pp. 1–8, 2019.
[5] S. B. Pawar and B. Thorat. Cfd simulation of taylor–couette flow in scraped surface heat exchanger. *Chemical engineering research design*, vol. 90, n. 3, pp. 313–322, 2012.
[6] Y. Park, L. Forney, J. Kim, and A. Skelland. Optimum emulsion liquid membranes stabilized by non-newtonian conversion in taylor–couette flow. *Chemical engineering science*, vol. 59, n. 24, pp. 5725–5734, 2004.
[7] S. J. Curran and R. A. Black. Oxygen transport and cell viability in an annular flow bioreactor: Comparison of laminar couette and taylor-vortex flow regimes. *Biotechnology and bioengineering*, vol. 89, n. 7, pp. 766–774, 2005.
[8] D. Paghdar, S. Jogee, and K. Anupindi. Large-eddy simulation of counter-rotating taylor–couette flow: The effects of angular velocity and eccentricity. *The International journal of heat and fluid flow*, vol. 81, pp. 108514, 2020.
[9] D. Pirrò and M. Quadrio. Direct numerical simulation of turbulent taylor–couette flow. *European journal of mechanics, B, Fluids*, vol. 27, n. 5, pp. 552–566, 2008.
[10] S. Viazzo and S. Poncet. Numerical simulation of the flow stability in a high aspect ratio taylor–couette system submitted to a radial temperature gradient. *Computers fluids*, vol. 101, pp. 15–26, 2014.
[11] S. Mahmoudirad, E. Shirani, and F. Aloui. Study of circular couette flow, taylor vortex and wavy vortex regimes in couette–taylor flows with transient periodic oscillation of the inner cylinder—a computational fluid dynamics analysis. *Journal of the Brazilian Society of Mechanical Sciences and Engineering*, vol. 43, n. 12, 2021.
[12] A. J. Dubas, N. Bressloff, and S. Sharkh. Numerical modelling of rotor–stator interaction in rim driven thrusters. *Ocean engineering*, vol. 106, pp. 281–288, 2015.
[13] M. L. Hosain, R. Bel Fdhila, and K. Rönnberg. Taylor-couette flow and transient heat transfer inside the annulus air-gap of rotating electrical machines. *Applied energy*, vol. 207, pp. 624–633, 2017.
[14] I. B. Celik, U. Ghia, P. J. Roache, C. J. Freitas, H. Coleman, and P. E. Raad. Procedure for estimation and reporting of uncertainty due to discretization in cfd applications. *Journal of fluids engineering*, vol. 130, n. 7, pp. 78001, 2008.
[15] B. Martínez-Arias, J. Peixinho, O. Crumeyrolle, and I. Mutabazi. Effect of the number of vortices on the torque scaling in taylor-couette flow, 2014.